

## EFFECT OF FREQUENCY IN BENDER ELEMENT TESTS FOR A FINE VOLCANIC ASH

Mukteshwar GOBIN<sup>1</sup>, Noriyuki YASUFUKU<sup>2</sup>, Guojun LIU<sup>3</sup> & Ryohei ISHIKURA<sup>4</sup>

**Abstract:** The small strain shear modulus,  $G_{max}$  is a fundamental parameter for seismic analysis and design. Bender elements (BE) are routinely used to estimate the shear wave velocity of geomaterials, from which the  $G_{max}$  may then be evaluated. Given their increasing popularity, in the last decade the Japanese Geotechnical Society (JGS) and American Society for Testing and Materials (ASTM) proposed standards to harmonize and reduce the subjectivity previously noted in the interpretation of BE waveforms. However, the standard methods recommended by both JGS and ASTM, per se, should be considered as a good set of guidelines, since hitherto, no one technique may be universally applied to all materials. This study aimed at understanding the effect of frequency on the shear wave signals of very fine volcanic ash soils (fines content > 90%) with very high water content (>150%). Remoulded volcanic ash with nano-sized clay minerals like allophane were sampled from two sites affected by the 2016 Kumamoto Earthquake in Japan. BE tests were carried out on saturated soil specimens at different void ratios and frequencies. For comparison purposes, similar tests were also conducted on Toyoura sand. Owing to the damping nature of the ash, the output signals have mostly a lower frequency than the input waves. Moreover, the interference of “near field effects” was evident at low input frequencies, which affects the proper determination of the arrival time. By considering the relationship between input and output frequencies and the transfer functions of the BE-soil systems, the optimum input frequencies for this type of soil was estimated, together with the delimiting travel length to wavelength ratio.

**Keywords:** Bender element; frequency; geophysics.

### 1. Introduction

The small strain shear modulus,  $G_{max}$  is considered to be one of the most important soil parameters necessary in geotechnical earthquake engineering problems like seismic ground response analysis, seismic design of foundations and other embedded infrastructures (like tunnels), liquefaction susceptibility, evaluation of soil-structure interaction and so on. Following the contributions of Lawrence (1963), Shirley and Hampton (1978) and Dyvik and Madhus (1985) in particular, bender elements (BE) gradually gained prominence as an alternative and simpler way for evaluating  $G_{max}$  (from the estimated shear wave velocity,  $V_s$ ) compared to other laboratory methods like resonant columns (RC), torsional or triaxial cyclic tests. These piezoceramic transducers provide several advantages in that they can be incorporated in different equipment like oedometer or triaxial device and are essentially a non-destructive method of testing (Cai *et al.*, 2015).

However, the signals from BE may be affected by problems like crosstalk, installation conditions, near field effects and wave dispersion (Lee & Santamarina, 2005). While solutions have been proposed for many of these technical problems (Ferreira *et al.*, 2021), the subjectivity related to the interpretation of the waveforms and the choice of the input frequency remains an ongoing theme of research. This is exemplified for instance by the divergent results reported from the round robin exercise carried out under the aegis of the then Technical Committee (TC) 29 (now TC101) of the International Society for Soil Mechanics and Geotechnical Engineering, between 23 different institutions from 11 countries (Yamashita *et al.*, 2009). Despite using the same standard Toyoura sand, it was pointed out that among others the choice for arrival time and input frequency varied between laboratories. This exercise prompted researchers and standards organizations to pursue further studies to reduce this perceivable subjectivity. New methods were

<sup>1</sup> Ph.D. Student, Kyushu University, Fukuoka, Japan, muktesh01@yahoo.co.uk

<sup>2</sup> Professor, Kyushu University, Fukuoka, Japan

<sup>3</sup> Lecturer, Changshu Institute of Technology, Suzhou, People's Republic of China

<sup>4</sup> Associate Professor, Kyushu University, Fukuoka, Japan

proposed based on the frequency domain and cross-correlation methods in lieu of the more popular time domain method (Viana da Fonseca *et al.*, 2009; Airey & Mohsin, 2013). Nonetheless, these alternative approaches have yet to receive complete acceptance.

The outcomes from the round robin exercise also formed the basis of the Japanese Geotechnical Society Standards (JGS) 0544 (2011): Method for laboratory measurement of shear wave velocity of soils by bender element test. While providing many useful guidelines, Kawaguchi *et al.* (2016) aptly mentioned that given JGS 0544 (2011) was proposed based on results on Toyoura sand, it may not be universally applied to all materials. They further added that JGS 0544 (2011) did not specifically mention how the input frequencies are to be chosen, providing as selection criterion a rather wide range based on travel length to wavelength ratio. Following the example of JGS, the American Society for Testing and Materials came with ASTM D8295–19: Standard Test Method for Determination of Shear Wave Velocity and Initial Shear Modulus in Soil Specimens using Bender Elements. Similar to JGS 0544 (2011), ASTM D8295–19 was another step in the direction towards harmonizing the methods used to interpret the BE signals. Nevertheless, it somehow bears a generic nature, for the method for interpreting the waveforms and only suggests matching the frequencies of input and output signals.

Many a paper are published without providing details for the choice of input frequency and in some cases the magnitude of the latter is also not reported. Recently, interesting works by Dutta *et al.* (2019) provided an objective criteria for the selection of input frequencies using disk-shaped transducers on dry granular materials. Equally pertinent would be to assess the effects of frequency on not so well studied fine natural materials in saturated conditions (more complex behaviour compared to dry conditions as reported by Cai *et al.*, 2015).

This study thus aimed at providing further insights into the influence of input frequency in BE tests, using non-textbook and liquefaction resistant allophanic volcanic ashes, which are found in seismically active regions not limited to Japan (Gobin *et al.*, 2023). BE tests were conducted at different confining pressures, void ratios and frequencies on black allophanic volcanic ash collected from two areas in the south of Japan. For comparison purposes similar tests were also carried on Toyoura sand. Considering the waveforms and relationship between input and output frequencies together with the results of transfer functions of the BE-soil systems, the optimum frequencies for these soils could be evaluated for a reliable estimation of the shear wave velocity.

## 2. Test Material

Remoulded allophanic volcanic ash, known locally as kuroboku was collected from two sites in Kyushu Island, Japan, which had been affected by the 2016 Kumamoto Earthquake. This type of volcanic ash is abundant in Japan and contains the nano-sized minerals allophane and imogolite. Soil 1 was collected from Naoiri (Site 1) in Oita prefecture and Soil 2 was gathered at Tateno, adjacent to the Aso Bridge landslide spot (Site 2). The sampling map is shown in Figure 1 (a).

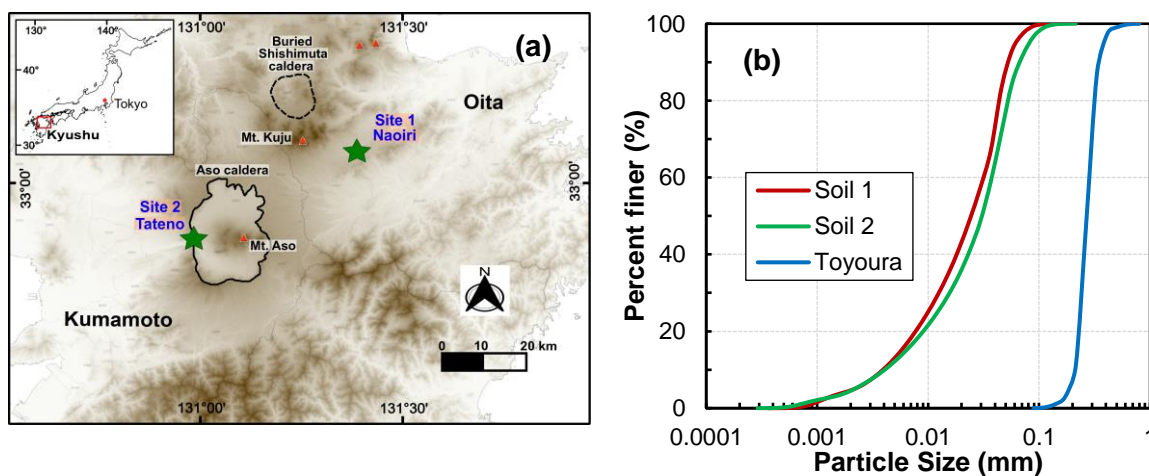


Figure 1. (a) Sampling locations (Source map from the Geospatial Information Authority of Japan, 2023); (b) Grain size distribution.

The grain size distribution of the soils determined using a laser diffraction particle size analyser (SALD-3103, Shimadzu) is shown in Figure 1 (b). The fines content of the allophanic volcanic

ashes exceed 90%. The basic properties of the soils are given in Table 1. It can be observed that the volcanic ashes are characterized by high natural water contents, high liquid and plastic limits (>130%). The volcanic ashes have “water of crystallization owing to their mineral composition. Thus, the water content of soils 1 and 2 was determined at 50°C (Gobin *et al.*, 2023).

Soil	Specific Gravity, $G_s$	Coefficient of Uniformity, $U_c$	Moisture content, $w$ (%)	Liquid limit, $LL$ (%)	Plastic limit, $PL$ (%)
Soil 1	2.172	8.034	160	170	144
Soil 2	2.390	9.216	157	183	135
Toyoura	2.646	1.368			

Table 1. Soil Properties.

### 3. Methodology

#### 3.1 Sample preparation and triaxial test procedures

Triaxial specimens 50 mm in diameter and 100 mm in height were prepared using the moist tamping and air pluviation methods for the volcanic ashes and Toyoura sand respectively. To saturate the specimens carbon dioxide (CO<sub>2</sub>) was percolated through the soil specimens for about 45 minutes. After that de-aired water was passed through the samples. A backpressure of 200 kPa was finally applied to the soil samples. Saturation was considered to be complete when the Skempton pore pressure ratio was at least 0.95.

#### 3.2 Bender element testing

Figure 2 shows the schematic diagram of the testing equipment for studying vertically propagating and horizontally polarised shear waves (vh). The BEs are mounted within the platens of the triaxial device, with the top BE acting as transmitter and the bottom one acting as receiver. Other ancillary equipment included a function generator (NF Digital Function Generator, DF1906), an amplifier (T-HVA03 High Voltage Amplifier - Turtle Industry Co., Ltd) and a digital oscilloscope (Iwatsu Digital Oscilloscope, DS-5105B).

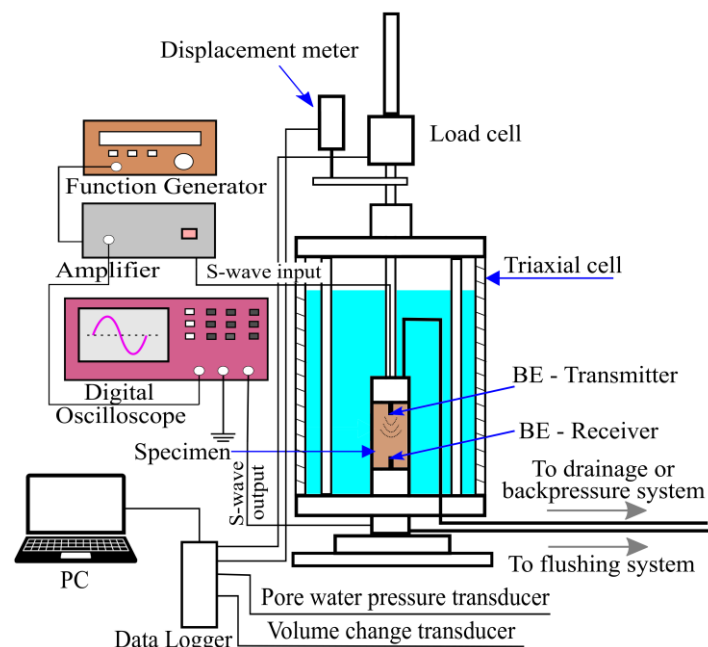


Figure 2. Simplified schematic diagram of testing equipment.

BE tests were performed at various time intervals after the end of the consolidation stage, at effective confining stresses ( $\sigma'$ ) between 50 and 200 kPa. The height and volume changes for the saturated specimens were captured by the linear variable differential transformer and volume gauge transducer respectively. Sine waves with a broad range of frequencies (2-20 kHz for the

volcanic ashes and 1-50 kHz for Toyoura sand) were used as input signals for a proper assessment of the effect of frequency.

### 3.3 Interpretation of waveform

Figure 3 shows the typical characteristics points plotted on a waveform of Soil 2. Nishimura (2006) used the characteristic points, S0-S1 in the start-start method for determining the first arrival point when studying the  $G_{max}$  of London clay. Based on tests on Toyoura sand, JGS 0544-2011 proposed the average of the start-start (S0-S2) and peak-peak points (P0-P1), discounting the system delay time. ASTM D8295–19 suggested using either S0-S2 or P0-P1 but they make allowance for other interpretation methods provided that the latter have shown to yield reliable results. Other methods may be more applicable to other types of soils or may not give reliable results over a wide range of frequencies. Therefore, in this research, the same approach as Nishimura (2006) was used to determine the travel time for the allophanic volcanic ash.

The shear velocity and stiffness may be evaluated using the following equations:

$$\text{Shear wave velocity, } V_s = \frac{L}{\Delta t} \quad (1)$$

$$\text{Shear stiffness, } G = \rho V_s^2 \quad (2)$$

where  $L$ : length between tip to tip of bender elements (mm);  $\Delta t$ : shear wave travel time (ms) and  $\rho$ : bulk density

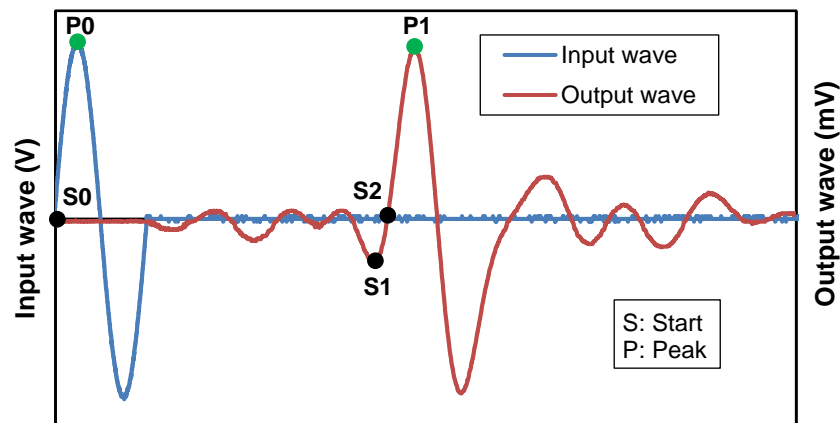


Figure 3. Nomenclature for signal interpretation.

## 4. Results and discussion

### 4.1 Near field effects

The dispersive phenomenon called near-field effects (NFE) which occurs due to compression waves or reflected shear waves influences the output signal and the determination of the arrival of shear wave in the BE tests (Youn *et al.*, 2008; Cai *et al.*, 2015; O'Donovan *et al.*, 2016). Figures 4(a) and (b) respectively show the waveforms generated for Soil 1 (void ratio,  $e = 3.68$ ;  $\sigma' = 50\text{kPa}$ ) and Soil 2 ( $e = 2.92$ ;  $\sigma' = 150\text{kPa}$ ) for different excitation frequencies. It can be observed that because of NFE, at low input frequencies ( $f_{in}$ ) especially, the determination of the first arrival time would be prone to error. The values obtained at  $f_{in}$  of 2 kHz seems to be most affected by NFE. For the volcanic ashes NFE decrease with increasing frequencies but beyond a certain threshold ( $\approx 6\text{-}8\text{kHz}$ ) no visible improvement is detected. Same observation was made for the other testing conditions which agrees with what Jovičić *et al.* (1996) found in their work.

As  $f_{in}$  increases, the wave length ( $\lambda$ ) decreases for a constant velocity. Ratios of travel distance ( $L$ ) to  $\lambda$  above which NFE would not be significant have been put forward. Depending on the materials tested, the ratios varied among the researchers, with Sanchez-Salinerro (1987), Arulnathan *et al.* (1998), Arroyo *et al.* (2003) and Leong *et al.* (2005) suggesting values of 2, 1, 1.6 and 3.33 respectively. JGS 0544-2011 also adopted the ratio of 2 as proposed by Sanchez-Salinerro.

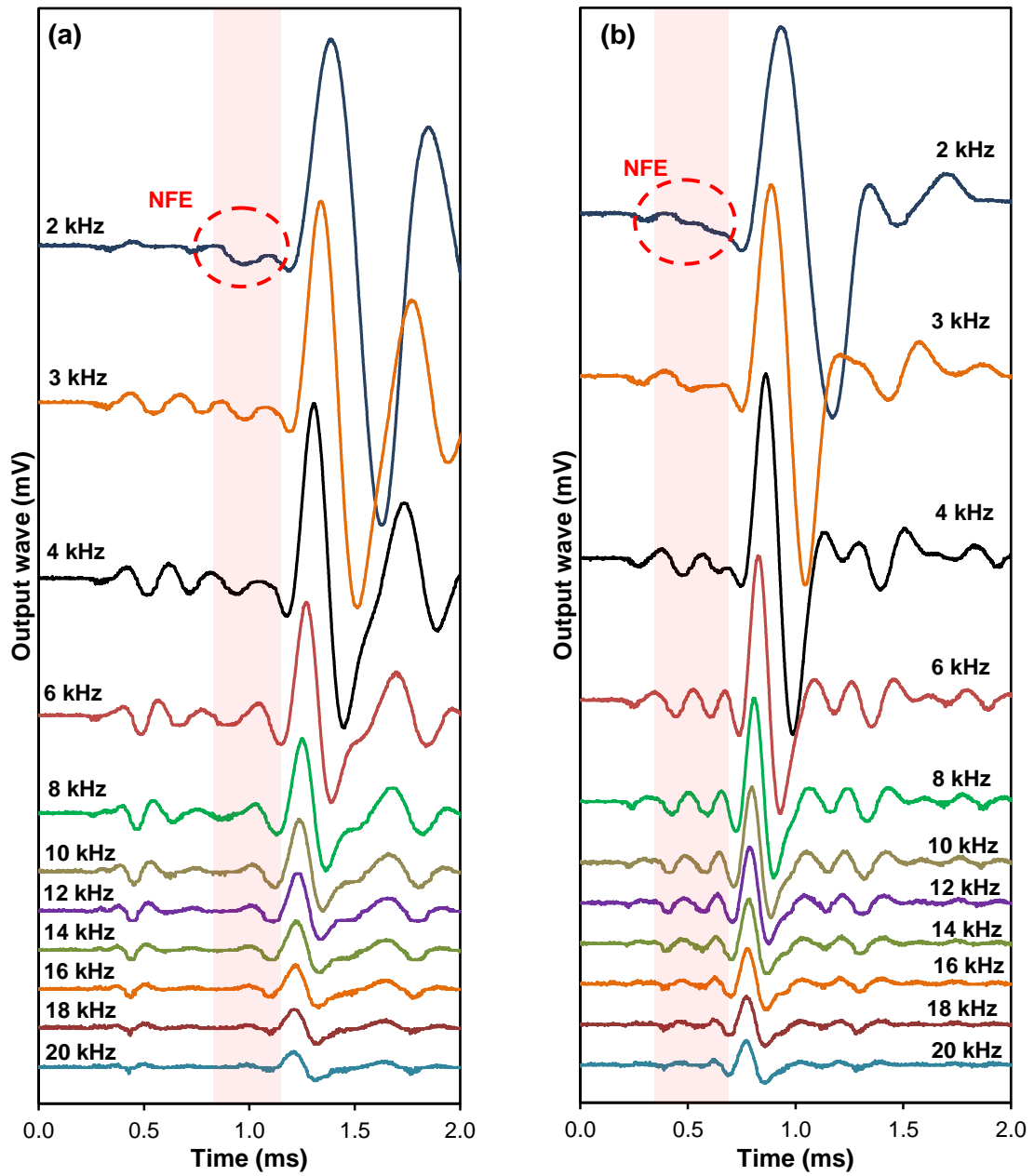


Figure 4. Output signals at different frequencies (a) Soil 1 ( $e=3.68, \sigma=50 \text{ kPa}$ ); (b) Soil 2 ( $e=2.92, \sigma=150 \text{ kPa}$ ).

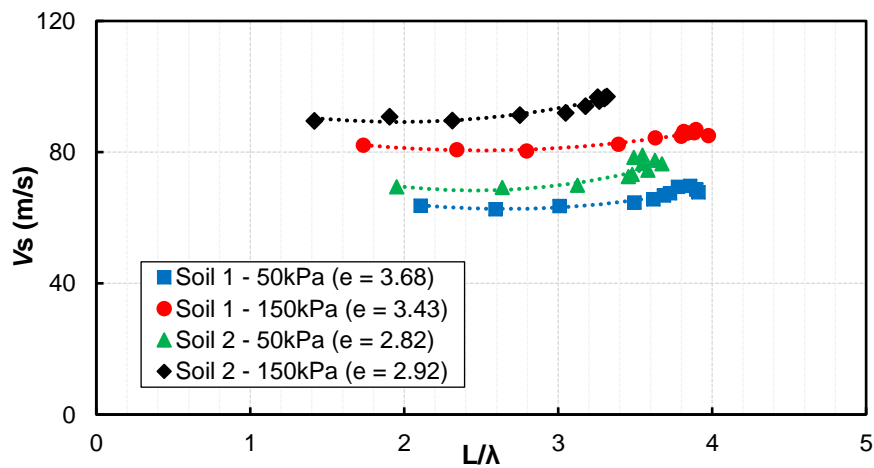


Figure 5. Influence of  $L/\lambda$  ratio on  $V_s$  at different effective confining pressures.

The influence of the ratio,  $L/\lambda$  on  $V_s$  is depicted in Figure 5. The results indicate that when  $f_{in}$  increases beyond about 3 kHz (near the resonant frequency), the  $V_s$  versus  $L/\lambda$  relationship for the volcanic ashes would tend to show a slight downward curvature. This means that the values of  $V_s$  between  $f_{in}$  of 3 and 8 kHz would be fairly similar. However, to minimize errors due to NFE it would be better to select  $f_{in}$  from 6 to 8 kHz. For effective confining pressures of 50 kPa,  $V_s$  values determined beyond  $f_{in}$  12 kHz display an irregular increase which may be attributed to higher noise or the values being determined beyond the maximum frequency that can be propagated through the samples. For the allophanic volcanic ashes, the acceptable range for  $L/\lambda$  lie between 2.7 to 3.8, with the lower and upper limits corresponding to  $\sigma'$  of 150 and 50 kPa respectively.

**4.2 Comparison of input ( $f_{in}$ ) and output frequency ( $f_{out}$ ) for determining optimum frequency**

The relationship between the input ( $f_{in}$ ) and output ( $f_{out}$ ) frequencies of the shear waves for the different soils studied is shown in Figure 6. It can be seen that irrespective of the material, void ratio, confining stress,  $f_{out}$  increases almost linearly at low  $f_{in}$ , before gradually tapering off to reach a threshold value. The decrease of the frequency as it travels through a soil sample has been attributed to the damping nature of the material. Moreover, this more or less linear trend noticed at low frequencies appears to correspond with the range of frequencies where NFE are predominant.

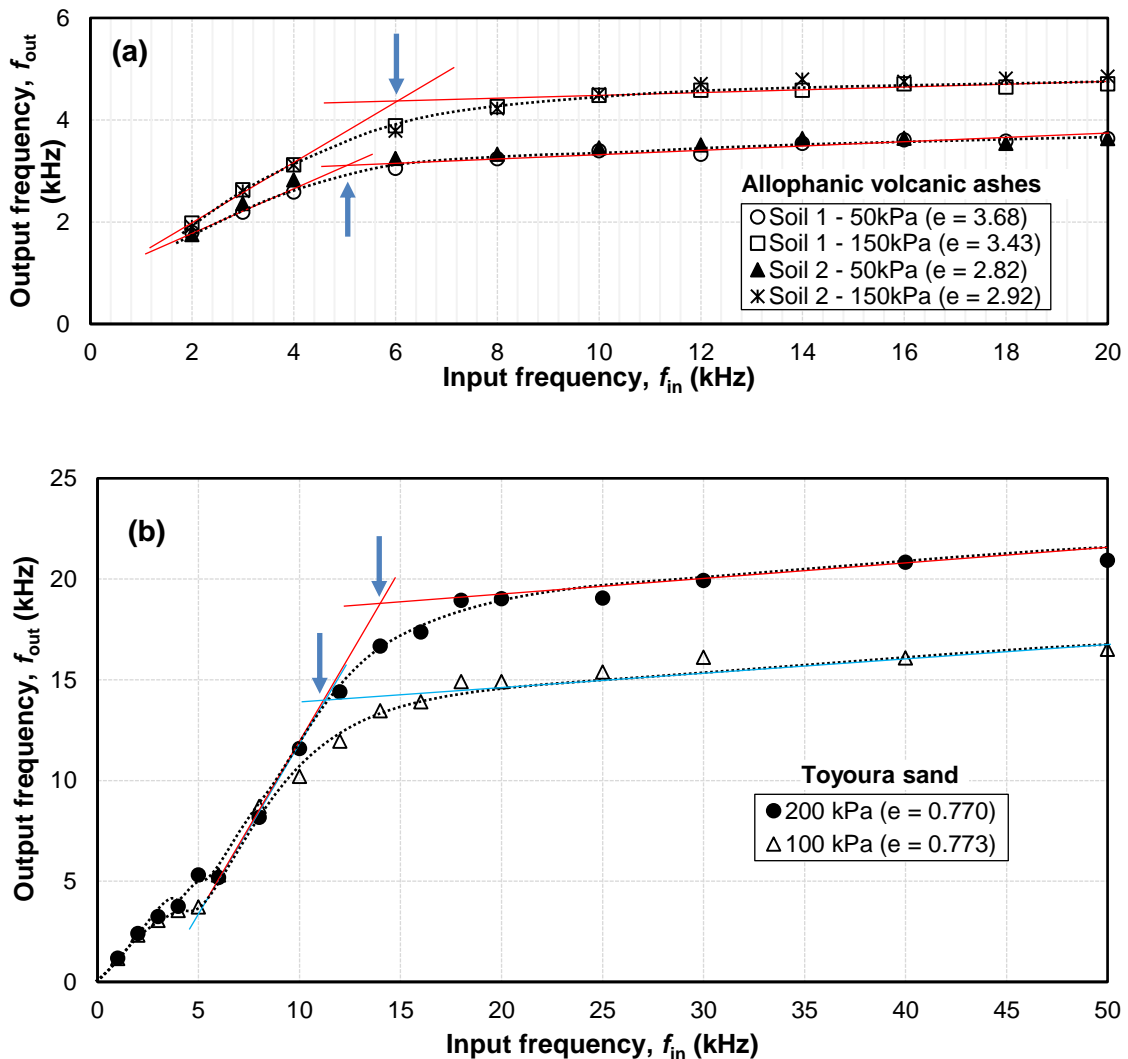


Figure 6. Relationship between input ( $f_{in}$ ) and output frequencies ( $f_{out}$ ) at different effective confining pressures (a) allophanic volcanic ashes; (b) Toyoura sand.

Importantly, it should be observed that  $f_{out}$  for the allophanic volcanic ashes is almost entirely lower than  $f_{in}$ , except at an effective confining pressure of 150kPa and input frequency of 2kHz, where they are nearly equal. This is in contrast with material of higher stiffness like Toyoura sand,

wherein  $f_{out}$  can be almost equal to  $f_{in}$  for a much broader range. Since it has been recommended to use an input frequency closer to the resonant frequency (Lee & Santamarina, 2005) and allowing for the reduction of NFE, it can therefore be deduced that the most appropriate  $f_{in}$  may be estimated around the point of inflection (as the curve concaves down) of an  $f_{in}$  versus  $f_{out}$  graph (indicated by arrows in Figure 6). For Toyoura sand ( $e = 0.773$ ), the point of inflection correspond to about 11.1 kHz for  $\sigma' = 100\text{kPa}$ . This roughly corresponds with the  $f_{in}$  of 10 kHz used by Gu *et al.* (2015) on saturated Toyoura sand ( $e = 0.797$ ). From this reasoning, this approximate method for determining  $f_{in}$  may also be extended to the allophanic volcanic ashes. From Figure 6 (a), it may be inferred that the range of 6 to 8 kHz seems most appropriate for the allophanic volcanic ashes, allowance being made for denser soil conditions than used in the present study. The input frequency of 6 kHz may probably be more reasonable at low effective confining stresses of 50kPa.

### 4.3 Transfer function for estimating the optimum input frequencies

A transfer function provides a means for measuring a system's dynamic response. It can be quantified through the gain factor that is the ratio of output to input amplitudes, which may be computed through fast Fourier transform algorithm. Figures 7(a), (b), (c) and (d) show the plots of gain factor for Soil 1 (void ratio,  $e = 3.68$ ;  $\sigma' = 50\text{kPa}$ ), Soil 1 ( $e = 3.43$ ;  $\sigma' = 150\text{kPa}$ ), Toyoura sand ( $e = 0.773$ ;  $\sigma' = 100\text{kPa}$ ) and Toyoura sand ( $e = 0.770$ ;  $\sigma' = 200\text{kPa}$ ) respectively.

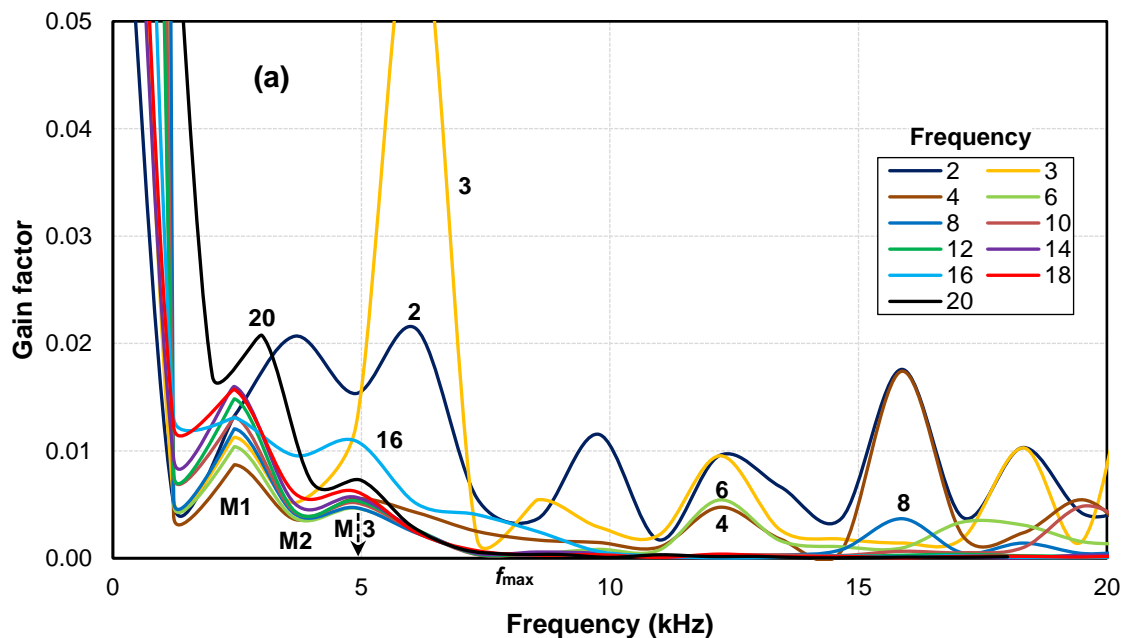


Figure 7. Gain factors (a) Soil 1 ( $e=3.68$ ,  $\sigma=50$  kPa)

From these figures, the multi-vibrational nature of the BE-soil system can be confirmed similar to Alvarado and Coop (2012). Each peak discerned therein denote a particular mode of vibration. The modes are excited to a greater extent at low  $f_{in}$  (closer to the resonant frequency) which is a direct consequence of the larger amplitudes of the received waves in this range. Moreover, it can be noticed that the allophanic volcanic ashes displayed lesser modes compared to the stiffer Toyoura sand. For both the volcanic ashes and Toyoura sand, their BE-soil system does not seem to follow a linear system at low frequencies.

The peak, M3 noted after the anti-resonance mode, M2 appears to represent the likely optimum input frequency. The first major mode, M1 probably represents the resonant frequency of the system. Considering the standard Toyoura sand ( $e = 0.773$ ;  $\sigma' = 100\text{kPa}$ ) in Figure 7(c), it can be further observed that the  $f_{in}$  corresponding to M3 (9.9 kHz) occurs around the point of inflection of the  $f_{in}$  versus  $f_{out}$  graph in Figure 6 (b). The M3 value coincides with the  $f_{in}$  of 10 kHz used by Gu *et al.* (2015) on saturated Toyoura sand ( $e = 0.797$ ). In addition, it may be pointed out that the optimum input frequencies estimated from the  $f_{in}$  versus  $f_{out}$  relationship in Figure 6 closely matches the M3 value for the allophanic volcanic ashes and very slightly exceed them for Toyoura sand.

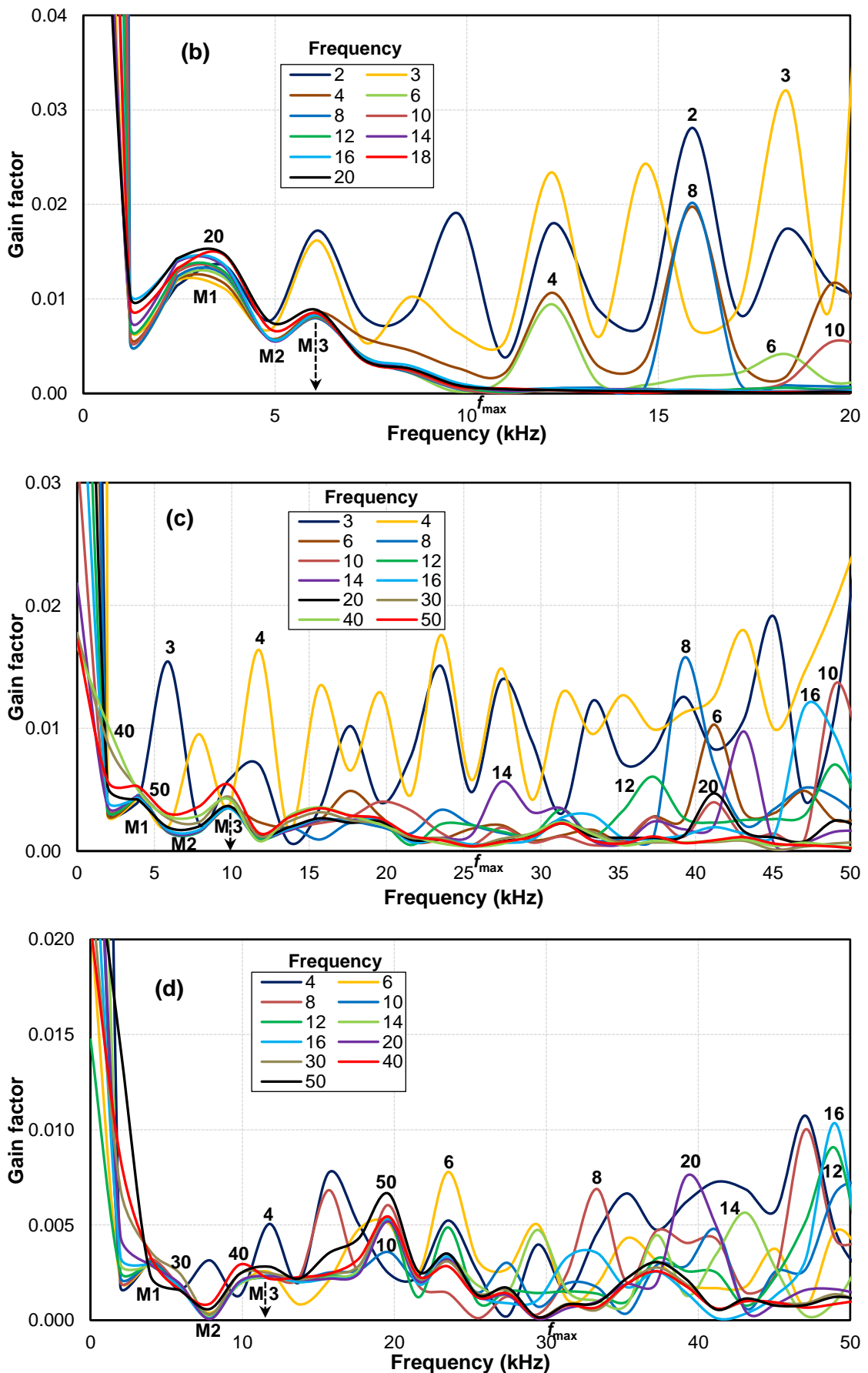


Figure 7(continued). Gain factors (b) Soil 1 ( $e=3.43, \sigma=150$  kPa); (c) Toyoura sand ( $e=0.773, \sigma=100$  kPa); (d) Toyoura sand ( $e=0.770, \sigma=200$  kPa)

The influence of confining stress on frequency is also confirmed by the migration of modes with increase in confining stress in the gain factor plots. For instance at an effective confining pressure of 100kPa, M3 corresponds to 9.9 kHz for Toyoura sand. Conversely at an effective confining pressure of 200kPa, M3 migrated to 11.3 kHz. For Soil 1, M3 moved from 4.9 kHz ( $\sigma' = 50\text{kPa}$ ) to 6.1 kHz ( $\sigma' = 150\text{kPa}$ ). For low to moderate effective confining stresses (50kPa to 200kPa) used in this study, probably usage of one input frequency would provide a very reasonable estimate of  $V_s$ . However, for larger increment in confining pressure, it may be advisable to increase  $f_{in}$ .

From the gain factor plots in Figure 7, an estimate of the maximum frequency ( $f_{max}$ ) that can be propagated through the sample can be made. The respective  $f_{max}$  values have been labelled in Figure 7. It can be deduced that  $f_{max}$  increases with the stiffness of the samples.

## 5. Conclusion

This study aimed at further understanding the effects of frequency in BE tests using allophanic volcanic ashes with high fines and water content, sampled from seismically active sites in Japan. Comparative BE tests on standard Toyoura sand were also carried out. The following are the main findings from this study:

- 1) Increasing excitation frequency minimizes the near-field effects, but beyond a certain frequency threshold ( $\approx 6\text{-}8$  kHz) no significant contribution in the reduction of near-field effects was observed for the allophanic volcanic ashes.
- 2) Although,  $V_s$  obtained between frequencies of 3 to 8 kHz for the allophanic soils did not vary by much, the range between 6 to 8 kHz is recommended to avoid errors related to near field effects.
- 3) The range for the ratio of  $L/\lambda$  between which near field effects are not significant, are quite narrow and varies with the effective confining stresses. The magnitude and range are both smaller at higher confining stresses.
- 4) Irrespective of the material, the optimum frequency could be estimated around the point of inflection (as the curve concaves down) of an  $f_{in}$  versus  $f_{out}$  graph.
- 5) Modal analysis was shown to provide an even more reliable estimate for the optimum input frequency as confirmed from results on standard Toyoura sand. Moreover, consideration for increase in  $f_{in}$  with effective confining stresses may also be evaluated using modal analysis.

## Acknowledgement

The first author is grateful to the Japanese Government (Monbukagakusho: MEXT) for sponsoring his studies. The first author also thank Dr. Troyee Dutta for kindly sharing his publications. The support of Kyushu University Library for procuring research materials and the help of Mr. Michio Nakashima, technical staff are also acknowledged.

## References

- Airey, D. and Mohsin, A.M., 2013. Evaluation of shear wave velocity from bender elements using cross-correlation. *Geotechnical testing journal*, 36(4), pp.506-514. <https://doi.org/10.1520/GTJ20120125>
- Alvarado, G. and Coop, M.R., 2012. On the performance of bender elements in triaxial tests. *Géotechnique*, 62(1), pp.1-17. <https://doi.org/10.1680/geot.7.00086>
- Arroyo, M., Muir Wood, D. and Greening, P.D., 2003. Source near-field effects and pulse tests in soil samples. *Géotechnique*, 53(3), pp.337-345. <https://doi.org/10.1680/geot.2003.53.3.337>
- Arulnathan, R., Boulanger, R. W., & Riemer, M. F., 1998. Analysis of bender element tests. *Geotechnical Testing Journal*, 21(2), 120-131. <https://doi.org/10.1520/GTJ10750J>
- ASTM International, 2019. Standard Test Method for Determination of Shear Wave Velocity and Initial Shear Modulus in Soil Specimens using Bender Elements. ASTM D8295–19. West Conshohocken, PA: ASTM International. <https://doi.org/10.1520/D8295-19>
- Cai, Y., Dong, Q., Wang, J., Gu, C., & Xu, C., 2015. Measurement of small strain shear modulus of clean and natural sands in saturated condition using bender element test. *Soil*

- Dynamics and Earthquake Engineering*. Elsevier, 76, pp. 100–110.  
<https://doi.org/10.1016/j.soildyn.2014.12.013>
- Dutta, T.T., Otsubo, M., Kuwano, R. and O'Sullivan, C., 2019. Stress wave velocity in soils: Apparent grain-size effect and optimum input frequencies. *Géotechnique Letters*, 9(4), pp.340-347. <https://doi.org/10.1680/jgele.18.00219>
- Dyvik, R. and Madshus, C., 1985, October. Lab measurements of  $G_{max}$  using bender elements. In *Advances in the art of testing soils under cyclic conditions* (pp. 186-196). ASCE.
- Ferreira, C., Diaz-Duran, F., da Fonseca, A.V. and Cascante, G., 2021. New approach to concurrent  $V_s$  and  $V_p$  measurements using bender elements. *Geotechnical Testing Journal*, 44(6). <https://doi.org/10.1520/GTJ20200207>
- Geospatial Information Authority of Japan, 2023. GSI Map. (in [Japanese]), [Online]. Available at: <https://maps.gsi.go.jp/> (Accessed February 11<sup>th</sup>, 2023).
- Gobin, M., Yasufuku, N., Liu, G., Watanabe, M. and Ishikura, R., 2023. Small strain stiffness, microstructure and other characteristics of an allophanic volcanic ash. *Engineering Geology*, 313, p.106967. <https://doi.org/10.1016/j.enggeo.2022.106967>
- Gu, X., Yang, J., Huang, M. and Gao, G., 2015. Bender element tests in dry and saturated sand: signal interpretation and result comparison. *Soils and Foundations*, 55(5), pp.951-962. <https://doi.org/10.1016/j.sandf.2015.09.002>
- Japanese Geotechnical Society Standards, 2011. JGS 0544: Method for laboratory measurement of shear wave velocity of soils by bender element test. Tokyo: The Japanese Geotechnical Society.
- Jovičić, V., Coop, M. R., & Simić, M., 1996. Objective criteria for determining  $G_{max}$  from bender element tests. *Géotechnique*, 46(2), 357-362. <https://doi.org/10.1680/geot.1996.46.2.357>
- Kawaguchi, T., Ogino, T., Yamashita, S. and Kawajiri, S., 2016. Identification method for travel time based on the time domain technique in bender element tests on sandy and clayey soils. *Soils and Foundations*, 56(5), pp.937-946. <https://doi.org/10.1016/j.sandf.2016.08.017>
- Lawrence, F.V. 1963. Propagation of ultrasonic waves through sand. Massachusetts Institute of Technology, Cambridge, Mass. Research Report R63–08
- Lee, J.S. and Santamarina, J.C., 2005. Bender elements: performance and signal interpretation. *Journal of geotechnical and geoenvironmental engineering*, 131(9), pp.1063-1070. [https://doi.org/10.1061/\(ASCE\)1090-0241\(2005\)131:9\(1063\)](https://doi.org/10.1061/(ASCE)1090-0241(2005)131:9(1063))
- Leong, E. C., Yeo, S. H., & Rahardjo, H., 2005. Measuring shear wave velocity using bender elements. *Geotechnical Testing Journal*, 28(5), 488-498. <https://doi.org/10.1520/GTJ12196>
- Nishimura, S., 2006. *Laboratory study on anisotropy of natural London Clay* (Doctoral dissertation, Imperial College London (University of London)).
- O'Donovan, J., Ibrahim, E., O'sullivan, C., Hamlin, S., Muir Wood, D. and Marketos, G., 2016. Micromechanics of seismic wave propagation in granular materials. *Granular Matter*, 18, pp.1-18. <https://doi.org/10.1007/s10035-015-0599-4>
- Sanchez-Salineró, I., 1987. *Analytical investigation of seismic methods used for engineering application* (Ph.D. dissertation, Austin: The University of Texas).
- Shirley, D. J., & Hampton, L. D., 1978. Shear-wave measurements in laboratory sediments. *The Journal of the Acoustical Society of America*, 63(2), 607-613. <https://doi.org/10.1121/1.381760>
- Viana da Fonseca, A., Ferreira, C. and Fahey, M., 2009. A framework interpreting bender element tests, combining time-domain and frequency-domain methods. *Geotechnical Testing Journal*, 32(2). <http://dx.doi.org/10.1520/GTJ100974>
- Yamashita, S., Kawaguchi, T., Nakata, Y., Mikami, T., Fujiwara, T., & Shibuya, S., 2009. Interpretation of international parallel test on the measurement of  $G_{max}$  using bender elements. *Soils and Foundations*, 49(4), pp. 631–650. <https://doi.org/10.3208/sandf.49.631>
- Youn, J. U., Choo, Y. W. and Kim, D. S., 2008. Measurement of small-strain shear modulus  $G_{max}$  of dry and saturated sands by bender element, resonant column, and torsional shear tests. *Canadian Geotechnical Journal*, 45(10), pp. 1426–1438. <https://doi.org/10.1139/T08-069>